Full-potential photoemission theory

M. Grass, J. Braun, and G. Borstel
Department of Physics, University of Osnabrück, D-4500 Osnabrück, Germany
(Received 25 November 1992)

The one-step model of photoemission is generalized to the case of space-filling potential cells of arbitrary shape. The resulting method differs from the usual muffin-tin formalism in an improved treatment of the single-center scattering, already successfully employed in full-potential Korringa-Kohn-Rostoker band-structure calculations. Finally it results in generalized matrix elements for the four contributions to the photocurrent that take the full nonspherical crystal potential into account. This generalized photoemission theory will be useful for the calculation of (inverse) photoemission spectra of ordered systems, such as pure elemental solids, compounds, and alloys, in a unified manner.

I. INTRODUCTION

The one-step model of photoemission[1,2] is an important and useful tool to interpret experimental data from angle-resolved ultraviolet photoemission (ARUPS) and angle-resolved bremsstrahlung isochromat spectroscopy (ARBIS). Moreover, it has advanced considerably in its range of applicability since its original formulation by Pendry and co-workers. In particular the enlargement to inverse photoemission[3,4] and the incorporation of a realistic model for the surface potential[4–6] as well as the inclusion of temperature[7,8] and relativistic[9,10] effects have strongly improved the number of applications. In addition an extension of the theory to materials with several atoms per unit cell is available.[11] The low-energy electron diffraction (LEED) theory, which is included in the one-step model of photoemission, has already been published in Ref. 12.

This model, which describes the photoemission process in a dynamical way, was originally formulated for muffin-tin potentials, which are spherical symmetric and nonzero only inside a sphere inscribed in the Wigner-Seitz cell, the so-called muffin-tin sphere. The muffin-tin approximation appears adequate for closed-packed systems, but it is a crude approximation for covalently bonded systems. In intermediate situations its adequacy depends on the accuracy sought. But even for those crystals, where this approximation is well justified, the restriction to the muffin-tin form is not desirable.

Growing interest in the electronic structure of complicated materials with more open structures, which are not well described by muffin-tin potentials, has led to the development of full-potential band-structure techniques, e.g., full-potential Korringa-Kohn-Rostoker (KKR),[13–21] full-potential linear muffin-tin orbital,[22,23] etc. These self-consistent calculations employ a space-filling crystal potential divided into cells of arbitrary shape, since contributions from regions outside the inscribed sphere are non-negligible and the potential inside the muffin-tin sphere deviates from the spherical average in most cases. A proper treatment of such systems within the one-step model of photoemission therefore also requires an employment of space-filling cell potentials, determined in self-consistent band-structure calculations on the basis of density-functional theory (DFT). An interpretation of photoemission spectra of more covalently complex systems will then be possible.

Since the widely used KKR theory for the calculation of band structures[24] has been generalized to the case of space-filling cell potentials of arbitrary shape,[13–21] the idea to develop a full-potential photoemission theory arose because these two theories are closely related in basic issues. As a basic requirement within both theories, the Schrödinger equation for a generally shaped nonspherical potential with proper boundary conditions must be solved. The method of solution is the expansion of the wave function inside the smallest sphere circumscribing the cell in a set of basis functions that are themselves integral equation solutions to Schrödinger's equation, the so-called "phase function" solutions. This basic idea was originally suggested by Williams and van Morgan[13] and led us to the generalization which is the subject of this paper.

A brief plan of the paper may be helpful: Section II presents the general theory of photoemission, calculated within the framework of many-body theory, and eludicates the remaining approximations made to transform the problem in a manageable form. Section III is devoted to the phase functional ansatz. It gives a short idea of how to use multiple-scattering theory in the case of a space-filling crystal potential. Moreover, the Schrödinger equation in the case of a single-cell potential is solved in a piecewise fashion by dividing space into a sphere containing the cell and the region outside, where the potential is zero. Section IV contains the generalization of some basic equations of photoemission theory to the full-potential case. In detail it is pointed out how the phase functional ansatz and therefore the picture of a nonspherical potential in a cell of arbitrary shape modifies the scattering solutions for a single cell, the scattering matrices for a single layer and the dipole operator. Finally, the four contributions to the photocurrent are calculated in Sec. V.

These derivations demonstrate that the phase functional ansatz enters the contributions in a straightforward manner, and though they are modified, the basic structure of the one-step model is kept. Section VI contains a short summary.

II. TEMPERATURE-DEPENDENT QUASIPARTICLE PHOTOEMISSION

The one-step model of (inverse) photoemission developed by Pendry and co-workers[1,2] describes the process of (inverse) photoemission in a dynamical way. The formula for the photocurrent, originally derived from Fermi's golden rule, can also be calculated on the basis of many-body theory.[8] Within this framework it is possible to give an abstract formulation of one- and two-particle spectroscopies such as ARUPS, ARBIS, Auger-electron spectroscopy, and appearance-potential spectroscopy in a consistent way.[25]

The central process relevant for one-particle spectroscopies like ARUPS (ARBIS) consists in the creation (annihilation) of an electron with wave vector $\mathbf{k}$ and energy E. Within the second quantization these spectroscopies may be described in an abstract manner by the operator $Z_r(r=\pm 1)$. The index r denotes the change in the total number of electrons within the system:

$$Z_1 = a_{\mathbf{k}}^{\dagger}\,, \tag{1}$$

$$Z_{-1} = a_{\mathbf{k}} \tag{2}$$

for ARBIS and ARUPS, respectively, where $a_{\mathbf{k}}^{\dagger}$ ($a_{\mathbf{k}}$) is the creation (annihilation) operator for an electron with wave vector $\mathbf{k}$ and energy E. The operator Z_r obeys the relation

$$Z_r^{\dagger} = Z_{-r}\,. \tag{3}$$

The intensity of the resulting radiation is directly related to the one-electron spectral density $A_r(E)$ by

$$I_r(E) = \frac{1}{1+e^{-\beta E}}\left(\frac{1}{\hbar}A_r(E)\right). \tag{4}$$

β denotes the Boltzmann factor. The one-electron spectral density $A_{\mathbf{k}}(E)$ for an electron with wave vector $\mathbf{k}$ and energy E is connected with the retarded one-electron Green function of the interacting system $G_{\mathbf{k}}(E) = \langle\langle a_{\mathbf{k}}; a_{\mathbf{k}}^{\dagger}\rangle\rangle_E^{\mathrm{ret}}$ via

$$\begin{aligned}\frac{1}{\hbar}A_{\mathbf{k}}(E) &= -\frac{1}{\hbar\pi}\,\mathrm{Im}\,\langle\langle a_{\mathbf{k}}; a_{\mathbf{k}}^{\dagger}\rangle\rangle_E^{\mathrm{ret}} \\ &= -\frac{1}{\hbar\pi}\,\mathrm{Im}\,\langle \mathbf{k}, E|G_{\mathbf{k}}(E)|\mathbf{k}, E\rangle\,. \end{aligned}\tag{5}$$

The energy E is referred to the Fermi energy E_F. The intensity of the resulting radiation for ARUPS (ARBIS) results by rewriting Eq. (4) as

$$I^{\mathrm{ARUPS}}(\mathbf{k},E) = \frac{1}{1+e^{-\beta E}} \times\left(-\frac{1}{\hbar\pi}\,Im\,\langle \mathbf{k}, E|G_{\mathbf{k}}(E)|\mathbf{k}, E\rangle\right) \quad (E<E_F)\,, \tag{6}$$

$$I^{\mathrm{ARBIS}}(\mathbf{k},E) = \frac{1}{1+e^{-\beta E}} \times\left(-\frac{1}{\hbar\pi}\,\mathrm{Im}\,\langle \mathbf{k}, E|G_{\mathbf{k}}(E)|\mathbf{k}, E\rangle\right) \quad (E>E_F)\,. \tag{7}$$

According to Eq. (3) both spectroscopies are determined by the same Green function $G_{\mathbf{k}}(E)$, which fulfills the Dyson equation

$$G_{\mathbf{k}}(E) = G_{\mathbf{k}}^0(E) + G_{\mathbf{k}}^0(E)\,\Sigma_{\mathbf{k}}(E)\,G_{\mathbf{k}}(E)\,. \tag{8}$$

$G_{\mathbf{k}}^0(E)$ denotes the one-electron Green function of the noninteracting system. Many-body correlation effects are taken into account by the complex self-energy $\Sigma_{\mathbf{k}}(E)$. The spectral density (5) can be expressed as a function of the real and imaginary part of the self-energy

$$A_{\mathbf{k}}(E) = -\frac{1}{\hbar\pi}\,\frac{\mathrm{Im}[\Sigma_{\mathbf{k}}(E)]}{\{E-\epsilon(\mathbf{k})-\mathrm{Re}[\Sigma_{\mathbf{k}}(E)]\}^2+\mathrm{Im}[\Sigma_{\mathbf{k}}(E)]^2}\,. \tag{9}$$

The one-particle energies $\epsilon(\mathbf{k})$ result from band-structure calculations based on the DFT.[26] The imaginary part of the self-energy contributes to the intensity of the resulting radiation by broadening the peaks appearing in the spectra. This effect corresponds to a finite lifetime of the initial state. The energetic positions of the peaks are shifted by the real part of the self-energy. For strongly correlated systems $\mathrm{Re}[\Sigma_{\mathbf{k}}(E)]$ exhibits a pronounced energy dependence. This results in the occurrence of additional peaks (satellites), which correspond to many-body effects.[27]

We have to keep in mind that the photocurrent for ARUPS (ARBIS) is not monitored by the intrinsic variables $\mathbf{k}$ and E of the final state, but by ϵ_f and $\mathbf{k}_{||}$, the single-particle energies of the outgoing (incoming) electron and the wave-vector component parallel to the surface. This is done by mapping the state $|\mathbf{k}, E\rangle$ with the help of first-order perturbation theory on a time-reversed LEED state $|\mathbf{k}_{||}, \epsilon_f\rangle$.[3,8] With the help of this projection the geometry of the experiment, the different densities of states for electrons (ARUPS) and photons (ARBIS) and the model of the semi-infinite crystal enter the theory:

$$|\mathbf{k}, E\rangle = \Delta^{+} G_2^{-}(E+\hbar\omega)|\mathbf{k}_{||}, \epsilon_f\rangle\,, \tag{10}$$

$$\langle \mathbf{k}, E| = \langle \mathbf{k}_{||}, \epsilon_f|G_2^{+}(E+\hbar\omega)\Delta\,. \tag{11}$$

$\hbar\omega$ denotes the energy of the electromagnetic wave field. The propagator of the excited high-energy electron $G_2^{\pm}(E+\hbar\omega)$ is derived from multiple-scattering techniques, while the operator Δ mediates the coupling to the electromagnetic field:

$$\Delta = \frac{e}{2mc}(\mathbf{A}\cdot\mathbf{p}+\mathbf{p}\cdot\mathbf{A}) - e\Phi + \frac{e^2}{2mc^2}\mathbf{A}\cdot\mathbf{A}\,. \tag{12}$$

$\mathbf{A}$ and Φ are the vector and scalar potential of the incident light field. $\mathbf{p}$ denotes the momentum operator. Using the well-justified dipole approximation,[1,27] we obtain Δ in its final form

$$\Delta \approx \frac{e}{mc}\mathbf{A}\cdot\mathbf{p}\,. \tag{13}$$

Inserting Eqs. (10) and (11) in (6) leads to the final expression for the photocurrent:

$$I^{\mathrm{ARUPS}}(\mathbf{k}_\parallel,\epsilon_f) = \frac{1}{e^{-\beta(\epsilon_f-\hbar\omega)}+1}\left(-\frac{1}{\hbar\pi}\mathrm{Im}\langle \mathbf{k}_\parallel,\epsilon_f|G_2^+(E+\hbar\omega)\Delta G_{\mathbf{k}}(E)\Delta^+ G_2^-(E+\hbar\omega)|\mathbf{k}_\parallel,\epsilon_f\rangle\right). \tag{14}$$

This formula is a proper generalization of the one-step model to temperature-dependent quasiparticle photoemission. Neglecting the temperature dependence and all many-body correlations ($\mathrm{Re}[\Sigma_{\mathbf{k}}(E)] = 0$), except lifetime effects ($\mathrm{Im}[\Sigma_{\mathbf{k}}(E)] \neq 0$), Eq. (14) reduces to the expression for the photocurrent, originally derived by Pendry and coworkers[1]

$$I^{\mathrm{ARUPS}}(\mathbf{k}_\parallel,\epsilon_f) = -\frac{1}{\hbar\pi}\mathrm{Im}\langle \mathbf{k}_\parallel,\epsilon_f|G_2^+(E+\omega)\Delta G_1^+(E)\Delta^+ G_2^-(E+\omega)|\mathbf{k}_\parallel,\epsilon_f\rangle\ . \tag{15}$$

In the following we will evaluate Pendry's formula for the photocurrent for a semi-infinite solid with a space-filling, nonspherical crystal potential and a realistic model for the surface potential.[5] The intensities of the electron (ARUPS) and photon current (ARBIS) are connected in a simple manner:[3]

$$I^{\mathrm{ARUPS}}(\mathbf{k}_\parallel,E+\hbar\omega) = \frac{2Ec^2\cos\theta}{\omega^2\cos\alpha} I^{\mathrm{ARBIS}}(\mathbf{k}_\parallel,E+\hbar\omega)\,. \tag{16}$$

α and θ denote the polar angles of the photons and electrons and $\epsilon_f = E+\hbar\omega$ the single-particle energy of the final state. Incorporation of relativistic effects and the temperature dependence into this model is discussed elsewhere.[7–10] The extension to several atoms per unit cell is straightforward.[11,12] These enlargements of the original theory are independent and an inclusion within the full-potential photoemission theory is easily possible.

Because of this reason we will concentrate on the evaluation of a nonrelativistic, temperature-independent, full-potential theory of (inverse) photoemission for solids with one atom per unit cell. In the following we will use atomic units ($\hbar = e = m = 1, c = 137.036$) and the positive z axis points inside the semi-infinite crystal. As usual the crystal is divided into identical layers parallel to the surface. Each of these layers consists, in the case of one atom per unit cell, of identical Wigner-Seitz cells, filled with the full nonspherical crystal potential.

For an explicit calculation of the photocurrent it is necessary to rewrite Eq. (15)

$$I(\mathbf{k}_\parallel,E+\omega) = -\frac{1}{\pi}\mathrm{Im}\int\int d\mathbf{r}\,d\mathbf{r}'\,\Phi(\mathbf{r},E+\omega) \times\Delta\, G_1^+(\mathbf{r},\mathbf{r}',E) \times\Delta^+\,\Phi^*(\mathbf{r}',E+\omega)\,. \tag{17}$$

$\Phi(\mathbf{r},E+\omega)$ denotes the multiple-scattered final-state wave field of the photoelectron

$$\Phi(\mathbf{r},E+\omega) = \langle \mathbf{k}_\parallel,E+\omega|G_2^+(E+\omega)|\mathbf{r}\rangle\,, \tag{18}$$

and $G_1^+(\mathbf{r},\mathbf{r}',E)$ is the Green function of the hole state

$$G_1^+(\mathbf{r},\mathbf{r}',E) = \langle \mathbf{r}|G_1^+(E)|\mathbf{r}'\rangle\,. \tag{19}$$

We will evaluate formula (17) for a space-filling crystal potential $V_c(\mathbf{r})$, which possesses the symmetry of some infinite regular lattice, using the structure of the method proposed by Hopkinson, Pendry, and Titterington.[2]

III. THE PHASE FUNCTIONAL APPROACH TO MULTIPLE-SCATTERING THEORY

In order to perform the calculation of the photocurrent for a solid with a space-filling, nonspherical potential, it is necessary to calculate the multiple-scattered initial- and final-state wave field in the whole crystal. For the solution of this problem we can use techniques which are well known from full-potential KKR calculations.[13–21] Especially the phase functional ansatz, which will be introduced in this section, was employed in the calculation of band structures from space-filling cell potentials.

Considering an advancing wave field entering a crystal with a space-filling potential, the problem of calculating the total scattered wave field at an arbitrary point $\mathbf{r}$ inside the solid can be solved by multiple-scattering theory. General principles of this theory state that each point of an incoming wave front is scattered independently at the potential in its vicinity. For this reason, it is possible to decompose the crystal potential into nonoverlapping cells of arbitrary shape. These cells act as independent scatterers. We are free to introduce a virtual interstitial region of infinitesimal volume that separates each of these cells. Since this region occupies zero volume, we choose the potential there to be zero.[17,20] Each of the independent scatterers act as a source of secondary outgoing waves, and it is the multiple scattering of all these secondary waves that determines the form of the whole scattered wave field.

All information concerning the scattering process is included in the scattering phases, resulting from matching conditions of the wave function at cell boundaries. There the wave functions inside the cell are matched to the solutions in the virtual interstitial region. Once we have determined the scattering phases, we can assume the scatterers as points and use the well-known technique of multiple scattering by dividing the crystal into layers and each layer into cells.

As a basic requirement, it remains to solve the Schrödinger equation for a single cell

$$[H + V(\mathbf{r}) - E]\Psi(\mathbf{r}, E) = 0 \,. \tag{20}$$

The potential consists of a cell with volume Ω, filled with the crystal potential $V_c(\mathbf{r})$, that is surrounded by zero potential:

$$V(\mathbf{r}), = \begin{cases} V_c(\mathbf{r}) \,, & \forall\, \mathbf{r} \in \Omega \\ 0 & \forall\, \mathbf{r} \in \Re^3 - \Omega \,. \end{cases} \tag{21}$$

A solid with one atom per unit cell is broken up into identical Wigner-Seitz cells. Within each cell there is just one singularity in the potential at the cell origin. For an atomiclike potential this singularity is less than v^{-2} and the potential is almost spherical symmetric near the origin.

Equation (20) can be solved in a piecewise fashion and the solution throughout the whole space is obtained by taking the proper matching conditions at the cell boundary into account. For $\mathbf{r} \in \Re^3 - \Omega$ Eq. (20) reduces to the Helmholtz equation. The solution $\Psi^0(\mathbf{r}, E)$ in all space is well known and analytic. For a given set of local basis functions $\Phi^\Omega_{L_1}(\mathbf{r}, E)$ the solution $\Psi^\Omega(\mathbf{r}, E)$ can be expanded inside the cell as[15,21]

$$\Psi^\Omega(\mathbf{r}, E) \;=\; \sum_{L_1} A_{L_1}(E)\, \Phi^\Omega_{L_1}(\mathbf{r}, E) \,. \tag{22}$$

L_1 denotes the composite labels $(l_1 m_1)$. The basis consists of those solutions of Eq. (20) that behave like free regular spherical waves at the origin:

$$\lim_{r \to 0} \Phi^\Omega_{L_1}(\mathbf{r}, E) \;=\; J_{L_1}(\mathbf{r}, E) \,. \tag{23}$$

$J_L(\mathbf{r}, E) = j_l(\kappa r) Y_l^m(\hat{\mathbf{r}})$ is a solid harmonic, which is regular at the origin, and $\kappa = \sqrt{2E}$. Therefore $\Psi^\Omega(\mathbf{r}, E)$ is well defined and analytic throughout Ω.[21] Because point-by-point matching of the wave functions $\Psi^\Omega(\mathbf{r}, E)$ and $\Psi^0(\mathbf{r}, E)$ across nonspherical cell boundaries is a troublesome way to meet the proper boundary condition

$$\Psi^\Omega(\mathbf{r}, E) = \Psi^0(\mathbf{r}, E) \,, \quad \forall\, \mathbf{r} \in \partial\Omega \,, \tag{24}$$

we make use of the analytic properties of these functions. Thus, we can match the analytic continuation of these wave functions at any surfaces, where the potential is zero, instead of matching them at cell boundaries.[18]

To obtain a solution that is expandable into spherical harmonics we choose a spherical surface. We match the solutions on a sphere circumscribing the whole cell, the so-called bounding sphere S (see Fig. 1). The center of the sphere coincides with the center of the atom inside the cell and therefore with the potential singularity. The equivalent boundary conditions are

$$\Psi^\Omega(\mathbf{r}, E) = \Psi^0(\mathbf{r}, E) \,, \quad \forall\, \mathbf{r} \in \partial S \,. \tag{25}$$

The basis functions $\Phi^\Omega_{L_1}(\mathbf{r}, E)$ will now be determined within the bounding sphere with proper boundary conditions on the surface ∂S and at the origin. We seek for local solutions of the Schrödinger equation

$$[H + V_S(\mathbf{r}) - E]\; \Phi^\Omega_{L_1}(\mathbf{r}, E) = 0 \,, \quad \forall\, \mathbf{r} \in S \tag{26}$$

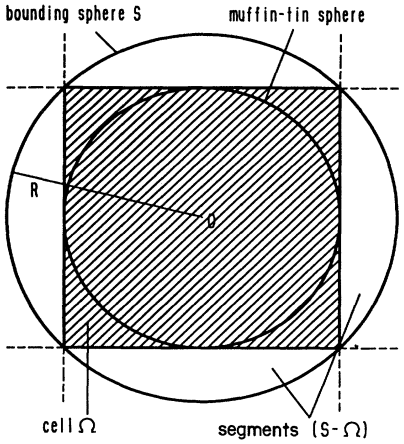

FIG. 1. Schematic representation of a typical cell of volume Ω, circumscribed by the bounding sphere S with radius R. The potential in the segments $(S - \Omega)$ is zero.

for a potential that is nonzero within the Wigner-Seitz cell and zero in the segments $(S - \Omega)$ (see Fig. 1)

$$V_S(\mathbf{r}) = \begin{cases} V_c(\mathbf{r}) \,, & \forall\, \mathbf{r} \in \Omega \\ 0 & \forall\, \mathbf{r} \in S - \Omega \,. \end{cases} \tag{27}$$

Using the nonspherical generalization of the phase functional ansatz of Calogero,[28] which was first used in full-potential band-structure calculations, we obtain solutions that form a set of complete, linearly independent functions, in terms of which an arbitrary solution of Eq. (26) can be expanded.[14] This phase functional ansatz yields a way of solving Schrödinger's equation for very general local potentials.[15,28] In our case the solutions are expandable in spherical harmonics:

$$\begin{aligned} \Phi^\Omega_{L_1}(\mathbf{r}, E) &= \sum_{L_2} Y_{L_2}(\hat{\mathbf{r}})\; \Phi^\Omega_{L_2 L_1}(r, E) \\ &= \sum_{L_2} J_{L_2}(\mathbf{r}, E)\; C^\Omega_{L_2 L_1}(r, E) \\ &\quad - N_{L_2}(\mathbf{r}, E)\; S^\Omega_{L_2 L_1}(r, E) \,. \end{aligned} \tag{28}$$

$N_L(\mathbf{r}, E) = n_l(\kappa r) Y_l^m(\hat{\mathbf{r}})$ is an irregular solid harmonic, and $C^\Omega_{L_2 L_1}(r, E)$ and $S^\Omega_{L_2 L_1}(r, E)$ are coefficient matrices. If the potential behaves reasonably smooth in the cell Ω without singularities except at the origin, we can define the following decomposition inside the bounding sphere:

$$V_S(\mathbf{r}) = \sum_{L_1} V_{L_1}(r)\; Y_{L_1}(\hat{\mathbf{r}}) \,, \tag{29}$$

with

$$V_{L_1}(r) = \int_{(4\pi)} d\hat{\mathbf{r}}\; V_S(\mathbf{r})\; Y^*_{L_1}(\hat{\mathbf{r}}) \,, \tag{30}$$

and $V_S(\mathbf{r})$ defined by Eq. (27). Inserting the phase functional ansatz (28) and the expansion of the potential in spherical harmonics (29) into the Schrödinger equation

(26) enables us to rewrite this equation as a coupled system of two linear differential equations for the coefficient matrices:

$$\frac{\partial}{\partial r}C^{\Omega}_{L_2L_1}(r,E) = -\,2\,\kappa\,r^2\,n_{l_2}(\kappa r) \times\sum_{L_3}\sum_{L_4}V_{L_3}(r)\,I_{L_2L_3L_4} \times\Phi^{\Omega}_{L_4L_1}(r,E)\;, \quad (31)$$

$$\frac{\partial}{\partial r}S^{\Omega}_{L_2L_1}(r,E) = -\,2\,\kappa\,r^2\,j_{l_2}(\kappa r) \times\sum_{L_3}\sum_{L_4}V_{L_3}(r)I_{L_2L_3L_4} \times\Phi^{\Omega}_{L_4L_1}(r,E)\;. \quad (32)$$

The coefficient $I_{L_2L_3L_4}$ describes the angular mixing:

$$I_{L_2L_3L_4} = \int_{(4\pi)} d\hat{\mathbf{r}}\;Y^*_{L_2}(\hat{\mathbf{r}})\;Y_{L_3}(\hat{\mathbf{r}})\;Y_{L_4}(\hat{\mathbf{r}})\;. \quad (33)$$

Including the correct boundary conditions at the origin (23),

$$C^{\Omega}_{L_2L_1}(0,E) = \delta_{L_2L_1}\;, \qquad S^{\Omega}_{L_2L_1}(0,E) = 0\;, \quad (34)$$

the following integral equations result:

$$C^{\Omega}_{L_2L_1}(r,E) = \delta_{L_2L_1} -2\kappa\int_0^r dr\int_{(4\pi)}d\Omega\;N^*_{L_2}(\mathbf{r},E) \times V_S(\mathbf{r})\;\Phi^{\Omega}_{L_1}(\mathbf{r},E)\;, \quad (35)$$

$$S^{\Omega}_{L_2L_1}(r,E) = -2\kappa\int_0^r dr\int_{(4\pi)}d\Omega\;J^*_{L_2}(\mathbf{r},E)\;V_S(\mathbf{r}) \times\Phi^{\Omega}_{L_1}(\mathbf{r},E)\;, \quad (36)$$

where $J^*_L(\mathbf{r},E) = j_l(\kappa r)Y^{m*}_l(\hat{\mathbf{r}})$ and $N^*_L(\mathbf{r},E) = n_l(\kappa r)Y^{m*}_l(\hat{\mathbf{r}})$ denote the complex-conjugate solid harmonics. Solutions can be determined by outward integration from the origin to the radius r for any potential less singular than v^{-2} at the origin. Integration out to the radius R of the bounding sphere S automatically determines the solution outside the bounding sphere ($\mathbf{r}\in\Re^3 - S$), where the coefficient matrices $C^{\Omega}_{L_2L_1}(R,E)$ and $S^{\Omega}_{L_2L_1}(R,E)$ are constant. The solutions of the Schrödinger equation are determined by the matrices C and S in the whole space. Inside the bounding sphere they are a function of r and outside constant. In the following we can drop the index Ω because solutions are in the whole space of the same structure. The coefficient matrices are the nonspherical equivalents of the scattering phase shifts $\cos(\delta_l)$ and $\sin(\delta_l)$ for the muffin-tin case. They determine the correct boundary conditions at the radius of the bounding sphere, and the scattering matrix can be directly extracted from their asymptotic form (see Sec. IV B).

Theoretically the L expansions (28) and (29) must be carried out to infinity. In practical calculations they are truncated at a reasonable value $l_{\max}$ that guarantees convergence for the basis functions $\Phi_{L_2L_1}(r)$. The value of $l_{\max}$ depends on the chosen geometry of the cell and the expansion of the potential inside the bounding sphere. These two conditions are closely related because the choice of the cell geometry determines the potential inside and finally the number of spherical harmonics needed in Eq. (29) to describe the potential with sufficient accuracy. First applications of the full-potential KKR theory to simple metals show strong convergence rates for $l_{\max}\le 4$. It is anticipated that calculations involving more open structures will not require a value of $l_{\max}$ higher than 6 or 8.[17] Moreover, the value of $l_{\max}$ depends on the excitation energy. For example, $l_{\max}=4$ is a good value for calculating ARUPS spectra in the energy range from $\hbar\omega = 0-40$ eV.

A problem that arises in practical calculations of the wave functions is the abrupt truncation of the potential at cell boundaries. Because of this truncation high nonspherical parts enter the expansion of the potential for large values of r, which cause convergence problems in the L expansion of the phase functions. Therefore Brown and Ciftan suggested a technique for calculating these functions that avoids truncation of the potential.[14,15,29] They use the full, untruncated crystal potential within the whole bounding sphere to determine the radial wave functions $\Phi_{L_2L_1}(r)$. Finally they solve the integral equations (35)and (36) for the coefficient matrices with these wave functions, employing the truncated potential. It is required that the segments ($S-\Omega$) do not contain any singularities, but this can be realized by a reasonable decomposition of the crystal potential in cells. The solutions calculated with the help of this technique built an identical set of basis functions to those obtained via direct calculations dealing with the truncated potential, since the boundary conditions at the origin are identical.[30] Moreover, they exhibit a stronger convergence rate.[20]

We can now expand an arbitrary solution $\Psi(\mathbf{r},E)$ as a linear combination of the nonspherical phase functions. All information concerning the scattering process of an incoming wave field at a nonspherical potential of arbitrary shape is included in the coefficient matrices C and S. Though we used a different set of basis functions as in the muffin-tin case, we obtained a solution which has the same basic structure. Inclusion in the one-step model of photoemission will therefore be straightforward.

IV. BASIC FORMULAS OF THE FULL-POTENTIAL PHOTOEMISSION THEORY

In this section we present the way the phase functional ansatz enters several basic formulas of photoemission theory. Moreover, we will eludicate the differences of these quantities to those obtained in connection with muffin-tin potentials.[1,2,12] In Sec. IV A we describe how scattering by a single Wigner-Seitz cell takes place and the way the irregular solution of the Schrödinger equation is determined. The scattering matrix for a single layer is introduced in Sec. IV B, and in Sec. IV C we describe the

generalized dipole operator that mediates the coupling of the high- and low-energy wave field in the full-potential case.

A. Scattering by a single cell

We already described in the preceding section the manner, in which the Schrödinger equation for a single Wigner-Seitz cell surrounded by zero potential is solved. This solution enables us to predict how incident electrons will move inside the bounding sphere. Once the incident wave is given, we are able to calculate the total wave function, incident and scattered, in all space.

The solution outside the bounding sphere (28) may be expressed in the form

$$\Phi_{L_1}(\mathbf{r},E) = \frac{1}{2}\sum_{L_2} H^{(1)}_{L_2}(\mathbf{r},E)\, U_{L_2L_1}(R,E) + H^{(2)}_{L_2}(\mathbf{r},E)\, V_{L_2L_1}(R,E)\ . \tag{37}$$

$H^{(1,2)}_L(\mathbf{r},E) = h^{(1,2)}_l(\kappa r)Y^m_l(\hat{\mathbf{r}})$ denote the spherical Hankel functions. Their asymptotic behavior leads us to identify the two parts of the expression as an outgoing and incoming wave. The coeffiecient matrices U and V are given by

$$\begin{aligned} U_{L_2L_1}(R,E) &= C_{L_2L_1}(R,E) + i\, S_{L_2L_1}(R,E)\ , \\ V_{L_2L_1}(R,E) &= C_{L_2L_1}(R,E) - i\, S_{L_2L_1}(R,E)\ . \end{aligned} \tag{38}$$

We can decompose (37) into unscattered $\Phi^0_{L_1}(\mathbf{r},E)$ and scattered $\Phi^s_{L_1}(\mathbf{r},E)$ components:

$$\Phi_{L_1}(\mathbf{r},E) = \Phi^0_{L_1}(\mathbf{r},E) + \Phi^s_{L_1}(\mathbf{r},E)\ , \tag{39}$$

$$\Phi^0_{L_1}(\mathbf{r},E) = \sum_{L_2} J_{L_2}(\mathbf{r},E)\, V_{L_2L_1}(R,E)\ , \tag{40}$$

$$\Phi^s_{L_1}(\mathbf{r},E) = \sum_{L_2}\sum_{L_3} H^{(1)}_{L_3}(\mathbf{r},E)\, \Gamma_{L_3L_2}(R,E)\, V_{L_2L_1}(R,E)\ . \tag{41}$$

$\Gamma_{L_3L_2}(R,E)$ is the scattering matrix for the cell:

$$\Gamma_{L_3L_2}(R,E) = \frac{1}{2}\left(\sum_{L_4} U_{L_3L_4}(R,E)V^{-1}_{L_4L_2}(R,E) - \delta_{L_3L_2}\right)\ . \tag{42}$$

If the potential happens to be zero inside as well as outside the bounding sphere—the nonscattering case—the matrix product UV^{-1} turns into the unit matrix. Therefore the scattering matrix and the scattered component of the wave function vanishes. $\Gamma_{L_3L_2}(R,E)$ is the nonspherical equivalent to the scattering phase $e^{2i\delta_l}$ in the muffin-tin case.

The irregular solution $\Phi^+_{L_1}(\mathbf{r},E)$ of the Schrödinger equation for $\mathbf{r} \in \Re^3 - S$ can be easily obtained from the scattered component (41) of the wave function:

$$\Phi^+_{L_1}(\mathbf{r},E) = \frac{1}{2}\sum_{L_2} V^{-1}_{L_1L_2}(R,E)\, H^{(1)}_{L_2}(\mathbf{r},E)\ . \tag{43}$$

We use again the phase functional ansatz to calculate the irregular wave function inside the bounding sphere ($\mathbf{r} \in S$):

$$\begin{aligned} \Phi^+_{L_1}(\mathbf{r},E) &= \sum_{L_2} \Phi^+_{L_1L_2}(\mathbf{r},E)\, Y_{L_2}(\hat{\mathbf{r}}) \\ &= \frac{1}{2}\sum_{L_2} \bar{U}_{L_1L_2}(r,E)\, H^{(1)}_{L_2}(\mathbf{r},E) \\ &\quad + \bar{V}_{L_1L_2}(r,E)\, H^{(2)}_{L_2}(\mathbf{r},E)\ . \end{aligned} \tag{44}$$

This solution to Eq. (26) is, however, irregular at the origin. The boundary conditions at the radius of the bounding sphere R are

$$\begin{aligned} \bar{U}_{L_1L_2}(R,E) &= V^{-1}_{L_1L_2}(R,E)\ , \\ \bar{V}_{L_1L_2}(R,E) &= 0\ . \end{aligned} \tag{45}$$

Inserting this ansatz (44) into the Schrödinger equation (26) yields analogous expressions for the coefficient matrices $\bar{U}$ and $\bar{V}$ that determine the irregular solution inside the bounding sphere:

$$\begin{aligned} \bar{U}_{L_1L_2}(r,E) &= V^{-1}_{L_1L_2}(R,E) \\ &\quad + 2i\kappa \int_r^R dr \int_{(4\pi)} d\Omega\, H^{(1)*}_{L_2}(\mathbf{r},E) \\ &\quad \times V_S(\mathbf{r})\, \Phi^+_{L_1}(\mathbf{r},E)\ , \\ \bar{V}_{L_1L_2}(r,E) &= -2i\kappa \int_r^R dr \int_{(4\pi)} d\Omega\, H^{(2)*}_{L_2}(\mathbf{r},E) \\ &\quad \times V_S(\mathbf{r})\, \Phi^+_{L_1}(\mathbf{r},E)\ , \end{aligned} \tag{46}$$

where $H^{(1,2)*}_L(\mathbf{r},E) = h^{(2,1)}_l(\kappa r)Y^{m*}_l(\hat{\mathbf{r}})$ denote complex-conjugate Hankel functions. These integral equations employ the truncated potential and therefore the convergence rate is worse than in the case of the regular solutions, calculated with the help of the technique suggested by Brown and Ciftan. Since the integration for the coefficient matrices $\bar{U}$ and $\bar{V}$ starts at the radius of the bounding sphere, we are not able to use this technique for the irregular solution. We are then left with two different values of $l_{\max}$ for the regular and the irregular solution. To take full advantage of the technique for calculating the phase functions introduced by Brown and Ciftan, one should use a different way to determine the irregular solution. The radial regular and irregular solution $\Phi_{L_2L_1}(r,E)$ and $\Phi^+_{L_1L_2}(r,E)$ to the Schrödinger equation meet a set of coupled Wronski-like relations, which reduce in the case of a muffin-tin potential to a well-known relation.[31] By solving this set of coupled differential equations one can also obtain the irregular solutions with an identical L expansion up to the same value of $l_{\max}$, as for the regular solution.

B. The scattering matrix for a single layer

Using the calculational scheme suggested by Pendry and co-workers, we have to determine the scattering matrix for a single layer. Once we know how an advancing planar wave field is scattered by a layer consisting of potential-filled Wigner-Seitz cells, we are able to calculate the multiple-scattered wave field between the layers in the whole crystal. For reasons of simplicity we will mark the energy dependence in the following by an index 1 (2) for the initial- (final-) state energy E ($E+\omega$). Starting point for the calculation of the transmission and reflection matrices of one layer is an advancing planar final-state wave field

$$\Psi^0_{2j}(\mathbf{r}) = \sum_{\mathbf{g}} W^+_{j\mathbf{g}}\, e^{i\mathbf{k}^+_{2\mathbf{g}}(\mathbf{r}-\mathbf{c}_j)} \,. \tag{47}$$

$\mathbf{c}_j$ denotes the position of the layer. $\mathbf{g}$ is a two-dimensional reciprocal lattice vector. $W^+_{j\mathbf{g}}$ stands for the amplitude of the advancing final-state wave field and $\mathbf{k}^+_{2\mathbf{g}}$ is its wave vector:

$$\mathbf{k}^{\pm}_{2\mathbf{g}} = \{-\mathbf{k}_{||}+\mathbf{g}\,,\ \pm\sqrt{2[(E+\omega)-V_{0r}-iV_{0i2}]\ -\ |-\mathbf{k}_{||}+\mathbf{g}|^2}\ \}\,. \tag{48}$$

$V_{0r} = E_F + W_F$, where W_F denotes the work function. By V_{0i2} we take the lifetime effects in the final state into account. This complex part in the inner potential may be identified with the imaginary part of the complex self-energy. We can expand this wave field into spherical waves as

$$\Psi^0_{2j}(\mathbf{r}) = \sum_{L_1}\sum_{\mathbf{g}} W^+_{j\mathbf{g}}\, 4\pi i^{l_1}\, Y^*_{L_1}(\hat{\mathbf{k}}^+_{2\mathbf{g}})\, j_{l_1}(\kappa_2 r)\, Y_{L_1}(\hat{\mathbf{r}}) \tag{49}$$

with

$$\kappa_2 = \sqrt{2(E+\omega-V_{0r}-iV_{0i2})}\,. \tag{50}$$

$\Psi^0_{2j}(\mathbf{r})$ corresponds to the unscattered part of the total wave field

$$\Psi^0_{2j}(\mathbf{r}) = \sum_{L_1} \Phi^0_{2L_1}(\mathbf{r})\, A^0_{2jL_1}\,, \tag{51}$$

where $\Phi^0_{2L_1}(\mathbf{r})$ is determined by formula (40). We obtain the coefficient $A^0_{2jL_1}$ by comparison of (51) and (49):

$$A^0_{2jL_1} = \sum_{L_2} V^{-1}_{2L_1L_2}(R) \sum_{\mathbf{g}} W^+_{j\mathbf{g}}\, 4\pi i^{l_2}\, Y^*_{L_2}(\hat{\mathbf{k}}^+_{2\mathbf{g}})\,. \tag{52}$$

Multiple-scattering within the layer is taken into account by Kambe's method.[12,32] As an extension to conventional LEED theory[12] we obtain in the full-potential case a generalized $\mathbf{X}$ matrix, correcting the coefficients $A^0_{2jL_1}$ concerning planar scattering within a layer:

$$A_{2jL_1} = \sum_{L_2}\sum_{L_3}\sum_{L_4} V^{-1}_{2L_1L_2}(R)\,(1-X)^{-1}_{2L_2L_3} \times V_{2L_3L_4}(R) A^0_{2jL_4}\,, \tag{53}$$

$$X_{2L_1L3} = \sum_j{}' \sum_{L_2} e^{i\mathbf{k}_{||}\mathbf{R}_j}\, G_{L_1L_2}(\mathbf{R}_o-\mathbf{R}_j)\,\Gamma_{2L_2L_3}(R). \tag{54}$$

The prime on the summation over j denotes that the unit cell at the origin has been omitted. An explicit expression for the matrix $G_{L_1L_2}$ is given in Ref. 12. Once we obtained the correct coefficients A_{2jL_1}, we are able to determine the scattered wave field from (41):

$$\Psi^s_{2j}(\mathbf{r}) = \sum_{L_1} \Phi^s_{2L_1}(\mathbf{r})\, A_{2jL_1} = \sum_{L_1}\sum_{L_2} H^{(1)}_{L_2}(\mathbf{r})\, W_{2L_2L_1}(R)\, A_{2jL_1}\,, \tag{55}$$

with

$$W_{2L_2L_1}(R) = \sum_{L_3} \Gamma_{2L_2L_3}(R)\, V_{2L_3L_1}(R) = i\, S_{2L_2L_1}(R)\,. \tag{56}$$

The amplitudes of the incoming and outgoing planar wave field are connected via the transmission and reflection matrices $T_{2\mathbf{g}\mathbf{g}'}$ and $R_{2\mathbf{g}\mathbf{g}'}$ for one layer:

$$W^-_{j\mathbf{g}} = \sum_{\mathbf{g}'} R_{2\mathbf{g}\mathbf{g}'}\, W^+_{j\mathbf{g}'}\,, \tag{57}$$

$$V^+_{j\mathbf{g}} = \sum_{\mathbf{g}'} T_{2\mathbf{g}\mathbf{g}'}\, W^+_{j\mathbf{g}'}\,. \tag{58}$$

We can calculate the transmission matrix from the scattered component of the whole wave field. Summing over all outgoing waves from cells within the layer and transforming to a plane-wave representation gives for the transmitted waves

$$\Psi^s_{2j}(\mathbf{r}) = \sum_{\mathbf{g}'} V^+_{j\mathbf{g}'}\, e^{i\mathbf{k}^+_{2\mathbf{g}'}(\mathbf{r}-\mathbf{c}_j)}\,. \tag{59}$$

We can rewrite this expression as

$$V^+_{j\mathbf{g}'} = \frac{1}{\mathcal{L}^2}\int d\mathbf{r}_{||}\, \Psi^s_{2j}(\mathbf{r})\, e^{-i\mathbf{k}^+_{2\mathbf{g}}(\mathbf{r}-\mathbf{c}_j)}\,, \tag{60}$$

where $\mathcal{L}^2$ denotes the area of unit cell of the layer. The transmission matrix can be identified by evaluating the integral (60) with the help of techniques suggested by Pendry[12] and by comparison with (58). We obtain

$$T_{2\mathbf{g}\mathbf{g}'} = \frac{8\pi^2}{\kappa_2\,\mathcal{L}^2\,|\mathbf{k}^+_{2\mathbf{g}_z}|} \sum_{L_1}\sum_{L_2}\sum_{L_3} i^{-l_1}\, Y_{L_1}(\hat{\mathbf{k}}^+_{2\mathbf{g}'})\,\Gamma_{2L_1L_2}(R)\,(1-X)^{-1}_{2L_2L_3} i^{l_3}\, Y^*_{L_3}(\hat{\mathbf{k}}^+_{2\mathbf{g}}) \ +\ \delta_{\mathbf{g}'\mathbf{g}}\,, \tag{61}$$

$$R_{2\mathbf{g}\mathbf{g}'} = \frac{8\pi^2}{\kappa_2 \mathcal{L}^2 |\mathbf{k}^+_{2\mathbf{g}_z}|} \sum_{L_1} \sum_{L_2} \sum_{L_3} i^{-l_1} Y_{L_1}(\hat{\mathbf{k}}^+_{2\mathbf{g}'}) \Gamma_{2L_1L_2}(R) (1-X)^{-1}_{2L_2L_3} i^{l_3} Y^*_{L_3}(\hat{\mathbf{k}}^-_{2\mathbf{g}}) . \quad (62)$$

It can be easily shown that the transmission and reflection matrix for one layer, consisting of cells filled with the full crystal potential (61) and (62), are the nonspherical generalizations of the matrices obtained in the muffin-tin case.[1] Replacing the coefficient matrix Γ by their spherical equivalent $\frac{1}{2}(e^{2i\delta_l} - 1)$ reduces Eqs. (61) and (62) to the expressions derived in the muffin-tin case.

Now we are able to calculate the multiple-scattered wave fields for the final-state electron moving inside a crystal with space-filling potential at an arbitrary point $\mathbf{r}$ inside the crystal. At this stage the full-potential LEED theory is complete.

C. The dipole operator

The basic process of photoemission consists in the excitation of an electron from an initial state (E) to a final state ($E+\omega$). This excitation is described by the dipole operator Δ (13) that mediates the coupling of the high- and low-energy wave field. As a consequence of conventional manipulations we get

$$\Delta^+(\mathbf{r}) = \frac{-i}{2\omega c} \mathbf{A}_0 \nabla V_S(\mathbf{r}) e^{-i\mathbf{q}\cdot\mathbf{r}} . \quad (63)$$

$\mathbf{q}$ denotes the wave vector of the photon field and $\mathbf{A}_0$ is the amplitude of the spatially constant vector potential. The potential $V_S(\mathbf{r})$ is defined inside the bounding sphere by (27), (29), and (30), where the potential is zero in the segments $(S-\Omega)$. Since regions where the potential is zero do not contribute to the photocurrent, we are allowed to expand the dipole operator in spherical harmonics throughout the bounding sphere:

$$\Delta^+(\mathbf{r}) = \frac{-i}{2\omega c} e^{-i\mathbf{q}\cdot\mathbf{r}} \sum_{L_1} \sum_{a=1}^{3} \Delta^{+a}_{L_1}(\mathbf{r}) . \quad (64)$$

The three components of the dipole operator are classified by their angular dependence:

$$\begin{aligned} \Delta^{+1}_{L_1}(\mathbf{r}) &= \Delta^{+1}_{L_1}(r)\, Y_{L_1}(\theta,\varphi) , \\ \Delta^{+2}_{L_1}(\mathbf{r}) &= \Delta^{+2}_{L_1}(r)\, Y_{L_1}(\theta,\varphi)\, \cot(\theta) , \\ \Delta^{+3}_{L_1}(\mathbf{r}) &= \Delta^{+3}_{L_1}(r)\, Y_{L_1}(\theta,\varphi)\, \sin^{-1}(\theta) . \end{aligned} \quad (65)$$

The radial parts have the following form:

$$\begin{aligned} \Delta^{+1}_{l_1m_1}(r) &= A_r \frac{\partial V_{l_1m_1}(r)}{\partial r} , \\ \Delta^{+2}_{l_1m_1}(r) &= A_\theta\, l_1 \frac{V_{l_1m_1}(r)}{r} , \\ \Delta^{+3}_{l_1m_1}(r) &= A_\theta \left(\frac{2l_1+3}{2l_1+1} (l_1+1)^2 - m_1^2 \right)^{1/2} \frac{V_{l_1+1\,m_1}(r)}{r} \\ &\quad + i A_\varphi m_1 \frac{V_{l_1m_1}(r)}{r} . \end{aligned} \quad (66)$$

This generalized dipole operator reduces for a spherical muffin-tin potential to the usual form, well known from standard photoemission theory.

V. THE FOUR CONTRIBUTIONS TO THE PHOTOCURRENT

From the preceding section we know, how to generalize the basic relations used in photoemission theory for the full-potential case. Since we were able to keep the complete structure of the one-step model, developed in connection with muffin-tin potentials, an evaluation of Eq. (17) in the well-known manner is possible. From the decomposition of the crystal in identical layers and a surface barrier, it results as a consequence of multiple-scattering theory that the total photocurrent is divided into four different contributions. Each contribution may be calculated separately and the sum over all four parts leads us finally to the total photocurrent.

A. The atomic contribution

We begin by calculating the atomic contribution. The final-state electron wave field Φ_{2j}, represented outside the crystal as a time-reversed LEED state, is propagated inside the solid. It is scattered in between and inside each layer of Wigner-Seitz cells. Inside each bounding sphere surrounding a cell the final-state electron wave field is coupled to the corresponding initial-state wave field by the dipole operator. The outgoing initial-state wave field is excited within the same bounding sphere and thus acts as a source of an outgoing high-energy wave field that propagates outside the crystal. On its way to the surface again all scattering events inside the complete half-infinite crystal are taken into account.

The advancing planar high-energy electron wave field at the jth layer is

$$\Phi^0_{2j}(\mathbf{r}) = \frac{1}{\mathcal{L}} \sum_{\mathbf{g}} \left(W^+_{j\mathbf{g}} e^{i\mathbf{k}^+_{2\mathbf{g}}(\mathbf{r}-\mathbf{c}_j)} + V^-_{j\mathbf{g}} e^{i\mathbf{k}^-_{2\mathbf{g}}(\mathbf{r}-\mathbf{c}_j)} \right) . \quad (67)$$

The amplitudes $W^+_{j\mathbf{g}}$ and $V^-_{j\mathbf{g}}$ are determined with the help of the layer-doubling method originally used in LEED calculations.[12] All coordinates are referred to the origin of the jth layer $\mathbf{c}_j$. Expanding this wave field in spherical harmonics, we obtain in analogy to (52) and (53) the coefficient of the whole multiple-scattered wave field inside the bounding sphere centered at $\mathbf{c}_j$

$$\begin{aligned} A_{2jL_1} = \sum_{L_2} \sum_{L_3} & V^{-1}_{2L_1L_2}(R) (1-X)^{-1}_{2L_2L_3} \\ & \times \sum_{\mathbf{g}} 4\pi i^{l_3} \left[W^+_{j\mathbf{g}} Y^*_{L_3}(\hat{\mathbf{k}}^+_{2\mathbf{g}}) \right. \\ & \left. + V^-_{j\mathbf{g}} Y^*_{L_3}(\hat{\mathbf{k}}^-_{2\mathbf{g}}) \right] . \end{aligned} \quad (68)$$

The total final-state wave field inside the bounding sphere consists of the scattered and the unscattered component

$$\Phi_{2j}(\mathbf{r}) = \frac{1}{\mathcal{L}} \sum_{L_1} \Phi_{2jL_1}(\mathbf{r})\, A_{2jL_1}$$
$$= \frac{1}{\mathcal{L}} \sum_{L_1} \sum_{L_2} Y_{L_2}(\hat{\mathbf{r}})\, [\Phi^0_{2jL_2L_1}(r) + \Phi^s_{2jL_2L_1}(r)\,] A_{2jL_1} \,. \tag{69}$$

The atomic Green function for a cell of arbirtrary shape filled with the nonspherical crystal potential is constructed from the regular (37) and irregular (44) solution of the Schrödinger equation (26):

$$G^+_{1j}(\mathbf{r},\mathbf{r}') = -4i\kappa_1 \sum_{L_1} \sum_{L_2} \sum_{L_3} Y_{L_2}(\hat{\mathbf{r}})\, Y^*_{L_3}(\hat{\mathbf{r}'})$$
$$\times [\Phi_{1jL_2L_1}(r)\, \Phi^+_{1jL_1L_3}(r')\, \Theta(r'-r) + \Phi_{1jL_3L_1}(r')\, \Phi^+_{1jL_1L_2}(r)\, \Theta(r-r')\,] \,, \tag{70}$$

with

$$\kappa_1 = \sqrt{2(E - V_{0r} - iV_{0i1})} \,, \tag{71}$$

where V_{0i1} denotes the complex part of the inner potential for the initial state. The dipole operator is defined by (64)–(66). For the atomic contribution we have to evaluate the following integral:

$$I^{\text{atomic}}(\mathbf{k}_\parallel, E+\omega)$$
$$= -\frac{1}{\pi} \text{Im} \sum_{j=2}^{n} \int_0^R d\mathbf{r} \int_0^R d\mathbf{r}'\, \Phi_{2j}(\mathbf{r})\, \Delta_j(\mathbf{r})\, G^+_{1j}(\mathbf{r},\mathbf{r}')$$
$$\times \Delta^+_j(\mathbf{r}') \Phi^*_{2j}(\mathbf{r}') \,. \tag{72}$$

The integration is carried out over the bounding sphere of radius R. The sum over the layers j runs up to a finite value n, depending on inelastic effects taken into account by the complex part of the self-energy. It starts with $n = 2$, because the surface potential barrier is interpreted as the first layer of the crystal and calculated as a separate contribution (see Sec. V D).

It is convenient to separate the radial parts of the integral from the angular parts. As a consequence of the nonspherical potential we get three different angular matrix elements. These result directly from the more complicated structure of the dipole operator:

$$D^1_{L_1L_2L_3} = \frac{1}{2\omega c}\, e^{i\mathbf{q}\cdot\mathbf{c}_j} \int_{(4\pi)} d\hat{\mathbf{r}}\, Y_{L_1}(\hat{\mathbf{r}})\, Y^*_{L_2}(\hat{\mathbf{r}})\, Y_{L_3}(\hat{\mathbf{r}}) \,,$$
$$D^2_{L_1L_2L_3} = \frac{1}{2\omega c}\, e^{i\mathbf{q}\cdot\mathbf{c}_j} \int_{(4\pi)} d\hat{\mathbf{r}}\, Y_{L_1}(\hat{\mathbf{r}})\, Y^*_{L_2}(\hat{\mathbf{r}})\, Y_{L_3}(\hat{\mathbf{r}}) \cot(\theta) \,, \tag{73}$$
$$D^3_{L_1L_2L_3} = \frac{1}{2\omega c}\, e^{i\mathbf{q}\cdot\mathbf{c}_j} \int_{(4\pi)} d\hat{\mathbf{r}}\, Y_{L_1}(\hat{\mathbf{r}})\, Y^*_{L_2}(\hat{\mathbf{r}})\, Y_{L_3}(\hat{\mathbf{r}}) \sin^{-1}(\theta)$$

The radial parts of the integral (72) are given by

$$M^{ab}_{jL_1\cdots L_9} = -4\kappa_1 \int_0^R r^2 dr \int_0^R r'^2 dr'\, \Phi_{2jL_2L_1}(r)\, \Delta^a_{jL_3}(r)$$
$$\times [\Phi_{1jL_4L_5}(r)\, \Phi^+_{1jL_5L_6}(r')\, \Theta(r'-r)$$
$$+ \Phi_{1jL_6L_5}(r')\, \Phi^+_{1jL_5L_4}(r)\, \Theta(r-r')\,] \Delta^{+b}_{jL_7}(r')\, \Phi^*_{2jL_8L_9}(r') \,. \tag{74}$$

Though the double radial integration is carried out to the radius of the bounding sphere, we still calculate the photocurrent from a Wigner-Seitz cell, because the potential is zero in the segments and thus does not contribute to the photocurrent. The indices a and b $(a, b = 1, 2, 3)$ belong to the three different radial components of the dipole operator (66). Therefore we get nine different types of energy-dependent radial matrix elements, each as a function of nine sets of quantum numbers L_i, expanded up to a reasonable high value of $l_{\max}$. The atomic contribution to the photocurrent is

$$I^{\text{atomic}}(\mathbf{k}_\parallel, E+\omega) = \text{Im} \left(\frac{-i}{\pi \mathcal{L}^2}\right) \sum_{j=2}^{n} \sum_{\Lambda_9} A_{2jL_1} \left\{ \sum_{a=1}^{3} \sum_{b=1}^{3} D^a_{jL_2L_3L_4}\, M^{ab}_{jL_1\cdots L_9}\, D^{b*}_{jL_6L_7L_8} \right\} A^*_{2jL_9} \,, \tag{75}$$

where Λ_9 denotes the set of composite labels $L_1 \cdots L_9$.

B. The intralayer contribution

The atomic contribution to the photocurrent is corrected by the intralayer contribution, which takes the multiple scattering of the outgoing initial-state wave field within a layer into account. Therefore Eq. (17) must be rewritten as

$$I^{\text{intra}}(\mathbf{k}_\parallel, E+\omega) = -\frac{1}{\pi}\text{Im}\sum_{j=2}^{n}\int_0^R d\mathbf{r}\;\Phi_{2j}(\mathbf{r})\;\Delta_j(\mathbf{r})\;\Psi_{1j}^{\text{intra}}(\mathbf{r})\;. \tag{76}$$

The wave function $\Psi_{1j}^{\text{intra}}(\mathbf{r})$ acts as a source of hole states:

$$\Psi_{1j}^{\text{intra}}(\mathbf{r}) = \int_0^R d\mathbf{r}'\;G_{1j}^{+}(\mathbf{r},\mathbf{r}')\;\Delta_j^{+}(\mathbf{r}')\;\Phi_{2j}^{*}(\mathbf{r}')\;. \tag{77}$$

Inserting the expression for the Green function $G_{1j}^{+}(\mathbf{r},\mathbf{r}')$, the dipole operator $\Delta_j^{+}(\mathbf{r}')$ and the final-state wave field $\Phi_{2j}^{*}(\mathbf{r})$ in Eq. (77) enables us to determine the outgoing initial-state wave field:

$$\Psi_{1j}^{0}(\mathbf{r}) = \frac{1}{\mathcal{L}}\sum_{L_1}\sum_{L_2}\sum_{L_3} B_{1jL_1}^{0}\;V_{1L_1L_2}(R)\;\Phi_{1jL_2L_3}^{+}(r)\;Y_{L_3}(\hat{\mathbf{r}})\;, \tag{78}$$

where the coefficient is defined by

$$\begin{aligned} B_{1jL_1}^{0} = -4\kappa_1 \sum_{L_2}\sum_{L_3}\sum_{L_4}\sum_{L_5}\sum_{L_6} A_{2jL_2}^{*} \int_0^R d\mathbf{r}'\;Y_{L_3}^{*}(\hat{\mathbf{r}}')\;\Phi_{2jL_3L_2}^{*}(r') \\ \times\frac{1}{2\omega c}\left[\Delta_{L_4}^{+1}(r') + \Delta_{L_4}^{+2}(r')\cot(\theta') + \Delta_{L_4}^{+3}(r')\sin^{-1}(\theta')\right] \\ \times Y_{L_4}(\hat{\mathbf{r}}')\;e^{i\mathbf{q}\cdot\mathbf{c}_j}\;Y_{L_5}^{*}(\hat{\mathbf{r}}')\;\Phi_{1jL_5L_6}(r')\;V_{1L_6L_1}^{-1}(R)\;. \end{aligned} \tag{79}$$

In the following we have to take into account that the outgoing initial-state wave field is scattered within the jth layer consisting of Wigner-Seitz cells. Therefore we introduce a virtual incoming initial-state wave field

$$\Psi_{1je}^{0}(\mathbf{r}) = \frac{1}{\mathcal{L}}\sum_{L_1}\sum_{L_2} Y_{L_2}(\hat{\mathbf{r}})\;\Phi_{1jL_2L_1}^{0}(r)\;A_{1jL_1}^{0}\;, \tag{80}$$

where $\Phi_{1jL_2L_1}^{0}(r)$ is defined by (40). The amplitudes of the virtual incoming and the outgoing initial-state wave field are connected by the following relation:

$$A_{1jL_1}^{0} = \frac{1}{2}\sum_{L_2} W_{1L_1L_2}^{-1}(R)\;B_{1jL_2}^{0}\;. \tag{81}$$

Now we are able to use the **X**-matrix formalism we already introduced[32] (see Sec. IV B) to take scattering within a layer into account:

$$\begin{aligned} B_{1jL_1} = \sum_{L_2}\sum_{L_3}\sum_{L_4} V_{1L_1L_2}^{-1}(R)\;(1-X)_{1L_2L_3}^{-1} \\ \times V_{1L_3L_4}(R)\;A_{1jL_4}^{0}\;. \end{aligned} \tag{82}$$

B_{1jL} denotes the coefficient of the total initial-state wave field, but for the calculation of the intralayer contribution of the photocurrent we just need the scattered component of this wave field. We obtain this by subtracting the virtual advancing wave field from the total initial-state wave field:

$$\Psi_{1j}^{\text{intra}}(\mathbf{r}) = \frac{1}{\mathcal{L}}\sum_{L_1}\sum_{L_2} Y_{L_2}(\hat{\mathbf{r}})\;\Phi_{1jL_2L_1}(r)\;B_{1jL_1}^{s}\;, \tag{83}$$

with

$$\begin{aligned} B_{1jL_1}^{s} = \frac{1}{2}\sum_{L_2}\sum_{L_3}\sum_{L_4} V_{1L_1L_2}^{-1}(R)\{\,(1-X)_{1L_2L_3}^{-1} \\ -\delta_{L_2L_3}\,\} \\ \times\Gamma_{1L_3L_4}^{-1}(R)\;B_{1jL_4}^{0}\;. \end{aligned} \tag{84}$$

To calculate the intralayer contribution to the photocurrent we have to substitute (64)–(66), (69), and (83) in Eq. (76). Separating this expression in angular (73) and radial parts, we obtain three types of single radial matrix elements:

$$M_{jL_1L_2L_3L_4L_5}^{a} = \int_0^R r^2 dr\;\Phi_{2jL_2L_1}(r)\;\Delta_{L_3}^{a}(r)\;\Phi_{1jL_4L_5}(r), \qquad a = 1,2,3\;. \tag{85}$$

The final expression for the intralayer contribution to the photocurrent is

$$I^{\text{intra}}(\mathbf{k}_\parallel, E+\omega) = \text{Im}\left(\frac{-i}{\pi\mathcal{L}^2}\right)\sum_{j=2}^{n}\sum_{\Lambda_5} A_{2jL_1}\left\{\sum_{a=1}^{3} M_{jL_1\cdots L_5}^{a}\;D_{jL_2L_3L_4}^{a*}\right\} B_{2jL_5}^{s}\;, \tag{86}$$

where the index Λ_5 denotes a set of composite labels $L_1 \cdots L_5$.

C. The interlayer contribution

Finally we have to take into account that the outgoing initial-state wave field is also scattered between the layers. Therefore, we obtain an additional contribution to the photocurrent arising from the outgoing initial-state wave field, multiple scattered between all layers.

Once again we use Eq. (76)

$$I^{\text{inter}}(\mathbf{k}_\parallel, E+\omega) = -\frac{1}{\pi}\text{Im} \sum_{j=2}^{n} \int_0^R d\mathbf{r}\, \Phi_{2j}(\mathbf{r})\, \Delta_j(\mathbf{r})\, \Psi_{1j}^{\text{inter}}(\mathbf{r}) \,. \quad (87)$$

We have to determine the initial-state wave field $\Psi_{1j}^{\text{inter}}(\mathbf{r})$, representing the hole state, multiple scattered in the whole semi-infinite crystal. The starting point is the outgoing initial-state wave field that is already corrected concerning intralayer scattering within the jth layer. Outside the bounding sphere it has the form

$$\Psi_{1j}^{s}(\mathbf{r}) = \frac{1}{\mathcal{L}} \sum_{L_1} \sum_{L_2} H_{L_2}^{(1)}(\mathbf{r})\, W_{1jL_2L_1}(R)\, B_{1jL_1} \,, \quad (88)$$

with the coefficient we already calculated in the preceding section:

$$B_{1jL_1} = \frac{1}{2} \sum_{L_2} \sum_{L_3} \sum_{L_4} V_{1L_1L_2}^{-1}(R)\, (1-X)_{1L_2L_3}^{-1} \times \Gamma_{1L_3L_4}^{-1}(R) B_{1jL_4}^{0} \,. \quad (89)$$

To calculate the interlayer scattering it is useful to expand this outgoing wave field into plane waves:

$$\Psi_{1j}^{s}(\mathbf{r}) = \frac{1}{\mathcal{L}} \sum_{\mathbf{g}} a_{j\mathbf{g}}^{\pm}\, e^{i\mathbf{k}_{1\mathbf{g}}^{\pm}(\mathbf{r}-\mathbf{c}_j)} \,. \quad (90)$$

$\mathbf{k}_{1\mathbf{g}}^{\pm}$ denotes the wave vector of the initial-state wave field

$$\mathbf{k}_{1\mathbf{g}}^{\pm} = \left(-\mathbf{k}_{||}+\mathbf{g}\,,\ \pm\sqrt{2[E-V_{0r}-iV_{0i1}] \;-\; |-\mathbf{k}_{||}+\mathbf{g}|^2}\ \right) . \quad (91)$$

The coefficients of this planar wave field leaving the jth layer are defined by

$$a_{j\mathbf{g}}^{\pm} = \frac{2\pi}{\mathcal{L}^2 \kappa_1 |k_{1\mathbf{g}_z}^{\pm}|} \sum_{L_1} \sum_{L_2} i^{-l_2}\, Y_{L_2}(\hat{\mathbf{k}}_{1\mathbf{g}}^{\pm}) \times W_{1jL_2L_1}(R)\, B_{1jL_1} \,. \quad (92)$$

With the help of the layer-doubling method[12] we are able to calculate the planar initial-state wave field advancing at the jth layer, multiple scattered between all layers:

$$\Psi_{1j}^{s}(\mathbf{r}) = \frac{1}{\mathcal{L}} \sum_{\mathbf{g}} \left(d_{j\mathbf{g}}^{+}\, e^{i\mathbf{k}_{1\mathbf{g}}^{+}(\mathbf{r}-\mathbf{c}_j)} + d_{j\mathbf{g}}^{-}\, e^{i\mathbf{k}_{1\mathbf{g}}^{-}(\mathbf{r}-\mathbf{c}_j)} \right) . \quad (93)$$

The coefficients of the advancing wave front $d_{j\mathbf{g}}^{\pm}$ can be easily determined from the coefficients of the outgoing wave front $a_{j\mathbf{g}}^{\pm}$, since we already determined the transmission and reflection matrices for a single layer (see Sec. IV B). Expansion in spherical waves leads us to the following expression for the whole initial-state wave field inside the bounding sphere:

$$\Psi_{1j}^{\text{inter}}(\mathbf{r}) = \frac{1}{\mathcal{L}} \sum_{L_1} \sum_{L_2} Y_{L_2}(\hat{\mathbf{r}})\, \Phi_{1jL_2L_1}(r)\, G_{1jL_1} \,, \quad (94)$$

where the coefficient G_{1jL_1} is already corrected concerning intralayer scattering within the jth layer:

$$G_{1jL_1} = \sum_{L_2} \sum_{L_3} V_{1L_1L_2}^{-1}(R)\, (1-X)_{1L_2L_3}^{-1} \times \sum_{\mathbf{g}} 4\pi i^{l_3} \left[d_{j\mathbf{g}}^{+}\, Y_{L_3}^{*}(\hat{\mathbf{k}}_{1\mathbf{g}}^{+}) + d_{j\mathbf{g}}^{-}\, Y_{L_3}^{*}(\hat{\mathbf{k}}_{1\mathbf{g}}^{-}) \right] . \quad (95)$$

Inserting the final-state wave field (69), the dipole operator, defined in Sec. IV C, as well as the wave field Ψ_{1j}^{inter} in Eq. (87), we obtain the interlayer contribution to the photocurrent. Separation in angular (73) and radial (85) parts lead us to the final expression

$$I^{\text{inter}}(\mathbf{k}_\parallel, E+\omega) = \text{Im}\left(\frac{-i}{\pi\mathcal{L}^2}\right) \sum_{j=2}^{n} \sum_{\Lambda_5} A_{2jL_1} \left\{ \sum_{a=1}^{3} M_{jL_1\cdots L_5}^{a}\, D_{jL_2L_3L_4}^{a*} \right\} G_{1jL_5} \,. \quad (96)$$

The index Λ_5 again denotes a set of composite labels $L_1 \cdots L_5$.

D. The surface contribution

The general theory of the surface contribution to the photocurrent in the one-step model is described in detail elsewhere.[4,6] Therefore we will concentrate in this section on the few differences arising in full-potential photoemission theory.

In general we have for the surface contribution to the photocurrent the formula

$$I^{\text{surf}}(\mathbf{k}_\parallel, E+\omega) = -\frac{1}{\pi}\text{Im} \int d\mathbf{r}\, \Phi_{21}(\mathbf{r})\, \Delta_1(\mathbf{r})\, \Psi_{11}^{\text{surf}}(\mathbf{r}) \,. \quad (97)$$

Since we consider the surface potential as the first layer of the crystal, the index j equals 1. $\Phi_{21}(\mathbf{r})$ then denotes the high-energy wave field at this layer. In the plane-wave expansion it can be calculated from Eq. (67), where the transmission and reflection matrices of the surface barrier for the final state are set to $T=1$ and $R=0$,[33]

$$\Phi_{21}(\mathbf{r}) = \frac{1}{\mathcal{L}} \sum_{\mathbf{g}} \left(V_{1\mathbf{g}}^{+} \, e^{i\mathbf{k}_{2\mathbf{g}}^{+}(\mathbf{r}-\mathbf{c}_1)} + V_{1\mathbf{g}}^{-} \, e^{i\mathbf{k}_{2\mathbf{g}}^{-}(\mathbf{r}-\mathbf{c}_1)} \right) . \tag{98}$$

The surface potential of a solid is described by an one-dimensional model barrier,[5] since corrugation effects in the surface potential seem to be of relative insignificance.[4,6] The dipole operator (63) for a one-dimensional surface potential $V_B(z)$ is given by

$$\Delta_1(\mathbf{r}) = \frac{A_z}{2\omega c} \, e^{-i\mathbf{q}\cdot\mathbf{r}} \, \frac{d}{dz} V_B(z) , \tag{99}$$

where A_z is the z component of the photon field. The complete initial-state wave field at the surface barrier results from standard manipulations,[1] and in the plane-wave representation we arrive at the following expression:

$$\begin{aligned} \Psi_{11}^{\mathrm{surf}}(\mathbf{r}) &= \langle \mathbf{r}| \, G_1^{+} \, \Delta_1^{+} \, G_2^{-} \, |\mathbf{k}_{||}, E+\omega\rangle \\ &= \frac{1}{\mathcal{L}} \sum_{\mathbf{g}} \left(a_{1\mathbf{g}}^{+} + r_{1\mathbf{g}} \, d_{1\mathbf{g}}^{-}\right) e^{i\mathbf{k}_{1\mathbf{g}}^{+}(\mathbf{r}-\mathbf{c}_1)} \\ &\quad + d_{1\mathbf{g}}^{-} e^{i\mathbf{k}_{1\mathbf{g}}^{-}(\mathbf{r}-\mathbf{c}_1)} . \end{aligned} \tag{100}$$

This is the expression where the full-potential ansatz enters the surface contribution, though we use a one-dimensional surface barrier. With the coefficient $a_{1\mathbf{g}}^{+}$ we take the hole state emitted by the surface barrier into account. It is already corrected concerning interlayer scattering inside the half-infinite crystal with space-filling potential. The intial-state wave field of the bulk region, emitted from the Wigner-Seitz cells and multiple scattered in the crystal with space-filling potential, enters the surface region via the coefficient $d_{1\mathbf{g}}^{-}$. It is calculated from Eq. (90) by the layer-doubling method. In the region of the varying surface potential we have an incoming component $d_{1\mathbf{g}}^{-}$ and an outgoing component $r_{1\mathbf{g}} d_{1\mathbf{g}}^{-}$ of this wave field.

According to the z dependence of the barrier potential, we have to calculate the initial- and final-state wave field numerically in the surface region. It follows for the initial state

$$\Psi_{11}^{\mathrm{surf}}(\mathbf{r}) = \frac{1}{\mathcal{L}} \sum_{\mathbf{g}} \psi_{1\mathbf{g}}(z) \, e^{i\mathbf{k}_{1\mathbf{g}||}(\mathbf{r}_{||}-\mathbf{c}_{1||})} , \tag{101}$$

with

$$\psi_{1\mathbf{g}}(c_{1z}) = a_{1\mathbf{g}}^{+} + r_{1\mathbf{g}} \, d_{1\mathbf{g}}^{-} + d_{1\mathbf{g}}^{-} , \tag{102}$$

and again for the final state

$$\Phi_{21}(\mathbf{r}) = \frac{1}{\mathcal{L}} \sum_{\mathbf{g}} \phi_{2\mathbf{g}}(z) \, e^{i\mathbf{k}_{2\mathbf{g}||}(\mathbf{r}-\mathbf{c}_{1||})} , \tag{103}$$

with

$$\phi_{2\mathbf{g}}(c_{1z}) = V_{1\mathbf{g}}^{+} + V_{1\mathbf{g}}^{-} . \tag{104}$$

Herein $\phi_{1\mathbf{g}}$ and $\psi_{2\mathbf{g}}$ denote the regular solutions of the Schrödinger equation for $V_B(z)$ in the range $-\infty < z < c_{1z}$. The value c_{1z} defines the point where the surface potential goes smoothly into $-V_{0r}$ inside the bulk crystal.

Inserting (101) and (103) into Eq. (97) and rewriting the surface contribution for the current, we arrive at the following expression:

$$I^{\mathrm{surf}}(\mathbf{k}_{||}, E+\omega) = -\frac{1}{\pi\mathcal{L}^2} \frac{A_z}{2\omega c} \, \mathrm{Im} \left(e^{i\mathbf{q}_{||}\cdot\mathbf{c}_{1||}} \sum_{\mathbf{g}} \int_{-\infty}^{c_{1z}} dz \, \phi_{2\mathbf{g}}(z) \, \frac{dV_B}{dz} \, \psi_{1\mathbf{g}}(z) \, e^{iq_z z} \right) . \tag{105}$$

The problem that remains is the calculation of the coefficient $a_{1\mathbf{g}}^{+}$, which belongs to the initial-state wave field emitted by the surface barrier. The initial-state matrix element $\langle \mathbf{r}|G_1^{+}\Delta^{+}G_2^{-}|\mathbf{k}_{||}, E+\omega\rangle$ can be manipulated to a form more appropriate to a direct calculation:

$$\begin{aligned} &\langle \mathbf{r}|G_1^{+}\Delta^{+}G_2^{-}|\mathbf{k}_{||}, E+\omega\rangle \\ &\quad = \int d\mathbf{r}' \langle \mathbf{r}| \, G_1^{+(0)} + G_1^{+(0)} \mathbf{r}_1 G_1^{+(0)} \, |\mathbf{r}'\rangle \\ &\qquad \times \Delta^{+} \langle \mathbf{r}'| \, G_2^{-} \, |\mathbf{k}_{||}, E+\omega\rangle , \end{aligned} \tag{106}$$

where $G_1^{+(0)}$ is the free-electron Green function for the initial state. After integrating over $d\mathbf{r}'_{||}$ in Eq. (106), we can describe the matrix element by a plane-wave expansion, which is valid in the region of our interest, namely between the surface barrier and the first bulk layer:

$$\langle \mathbf{r}|G_1^{+}\Delta^{+}G_2^{-}|\mathbf{k}_{||}, E+\omega\rangle = \frac{1}{\mathcal{L}} \sum_{\mathbf{g}} a_{1\mathbf{g}}^{+} \, e^{i\mathbf{k}_{1\mathbf{g}}^{+}(\mathbf{r}-\mathbf{c}_1)} , \tag{107}$$

with

$$a_{1\mathbf{g}}^{+} = -\frac{iA_z e^{-i\mathbf{q}\cdot\mathbf{c}_1}}{2\omega c k_{1\mathbf{g}z}^{+}} (1+r_{1\mathbf{g}}) \int_{-\infty}^{c_{1z}} dz \, e^{-i(q_z+k_{1\mathbf{g}z}^{+})(z-c_{1z})} \times \frac{dV_B}{dz} \, \phi_{2\mathbf{g}}(z) . \tag{108}$$

For a step barrier $V_B(z) = V_{0r}\Theta(z-c_{1z})$, where Θ is the unit step function, we obtain Pendry's result.[1]

In calculating the matrix element for the surface contribution we follow Pendry's original ansatz. The main effect from a z-dependent surface barrier results in a strong variation of the barrier reflection coefficient $r_{1\mathbf{g}}$. For that reason we use for the evaluation of this coefficient a potential model for $V_B(z)$, which has been introduced first by Rundgren and Malmström[33] in LEED calculations.

VI. SUMMARY

In this contribution we have derived a general technique for the calculation of (inverse) photoemission spectra within the one-step model that employs space-filling potential cells of arbitrary shape. Since we removed the muffin-tin approximation and therefore the geometrical restrictions for the potential, we are now left with stan-

dard approximations of photoemission theory. The treatment of muffin-tin potentials, e.g., for closed-packed crystals, within this generalized theory will still be possible. The method of solution contains all advantages of the original method of Pendry and co-workers. Moreover, the different enlargements of the original theory developed in recent years can also be incorporated in the full-potential case. Since we already demonstrated in this paper how to perform the calculation of (inverse) photoemission spectra for arbitrary ordered systems, employing a space-filling crystal potential and a realistic model for the surface potential, it remains to show explicitly how to perform the incorporation of relativistic and temperature effects. This will be done in a forthcoming publication.

The basic idea for the treatment of space-filling cell potentials in photoemission theory is the phase functional ansatz that enters the one-step model in a straightforward manner. It has been demonstrated in full-potential KKR calculations that an application of multiple-scattering theory to full-potential cell scattering is rigorously valid. The non-muffin-tin photoemission theory presented here demonstrates the feasibility of full-potential calculations of the photocurrent within the one-step model; the question whether the L expansions for strong covalently bonded systems are manageable with reasonable computational effort must be studied.

We are currently working on the computational implementation of this model.

ACKNOWLEDGEMENT

Financial support of this work by the Deutsche Forschungsgemeinschaft (SFB 225) is gratefully acknowledged.

[1] J. B. Pendry, Surf. Sci. **57**, 679 (1976).
[2] J. F. L. Hopkinson, J. B. Pendry, and D. J. Titterington, Comput. Phys. Commun. **19**, 69 (1980).
[3] J. B. Pendry, Phys. Rev. Lett. **45**, 1381 (1980).
[4] G. Borstel and G. Thörner, Surf. Sci. Rep. **8**, 1 (1988).
[5] G. Malmström and J. Rundgren, Comput. Phys. Commun. **19**, 263 (1980).
[6] M. Grass, J. Braun, and G. Borstel, J. Phys. C **5**, 599 (1993).
[7] C. G. Larson and J. B. Pendry, J. Phys. C **14**, 3089 (1981).
[8] J. Braun, G. Borstel, and W. Nolting, Phys. Rev. B **46**, 3510 (1992).
[9] G. Thörner and G. Borstel, Phys. Status Solidi B **126**, 617 (1984); J. Braun, G. Thörner, and G. Borstel, *ibid.* **130**, 643 (1985); **144**, 609 (1987).
[10] B. Ginatempo, P. J. Durham, and B.I. Gyorffy, J. Phys. C **1**, 6483 (1989).
[11] J. Braun (unpublished).
[12] J. B. Pendry, *Low Energy Electron Diffraction* (Academic, London, 1974).
[13] A. R. Williams and J. van Morgan, J. Phys. C **7**, 37 (1974).
[14] R. G. Brown and M. Ciftan, Phys. Rev. B **27**, 4564 (1983).
[15] R. G. Brown and M. Ciftan, *Condensed Matter Theories* (Plenum, New York, 1986), Vol. 1, p. 215.
[16] A. Gonis, X.-G. Zhang, and D. M. Nicholson, Phys. Rev. B **38**, 3564 (1988).
[17] A. Gonis, X.-G. Zhang, and D. M. Nicholson, Phys. Rev. B **40**, 947 (1989).
[18] X.-G. Zhang and A. Gonis, Phys. Rev. B **39**, 10373 (1989).
[19] X.-G. Zhang, A. Gonis, and J. M. MacLaren, Phys. Rev. B **40**, 3694 (1989).
[20] W. H. Butler and R. K. Nesbet, Phys. Rev. B **42**, 1518 (1990).
[21] W. H. Butler, A. Gonis, and X.-G. Zhang, Phys. Rev. B **45**, 11527 (1992).
[22] K. H. Weyrich, Phys. Rev. B **37**, 10269 (1988).
[23] M. Methfessel, C. O. Rodriguez, and O. K. Andersen, Phys. Rev. B **40**, 2009 (1989).
[24] W. Kohn and N. Rostoker, Phys. Rev. **94**, 1111 (1954).
[25] W. Nolting, Z. Phys. B **80**, 73 (1990).
[26] V. L. Moruzzi, J. F. Janak, and A. R. Williams, *Calculated Electronic Properties of Metals* (Pergamon, New York, 1978).
[27] G. Borstel, Appl. Phys. A **38**, 193 (1985).
[28] F. Calogero, *Variable Phase Approach to Potential Scattering* (Academic, New York, 1967).
[29] R. G. Brown and M. Ciftan, Phys. Rev. B **32**, 1343 (1985); **33**, 7937 (1986); R. G. Brown, J. Phys. B **21**, L309 (1988); R. G. Brown and M. Ciftan, Phys. Rev. B **39**, 10415 (1989).
[30] R. K. Nesbet, Phys. Rev. B **41**, 4948 (1990).
[31] A. Messiah, *Quantenmechanik* (de Gruyter, Berlin, 1976), Vol. 1.
[32] K. Kambe, Z. Naturforsch A **23**, 1280 (1968).
[33] J. Rundgren and G. Malmstöm, J. Phys. C **10**, 4671 (1977).